Blind Adaptive Multiuser Detection for Asynchronous Dual-Rate DS/CDMA Systems

Stefano Buzzi, *Member, IEEE*, Marco Lops, *Member, IEEE*, and Antonia M. Tulino

***Abstract*—In this paper, the authors consider an asynchronous direct-sequence code division multiple access (DS/CDMA) system wherein users are allowed to transmit their symbols at one out of two available data rates. Three possible access schemes are considered, namely, the variable spreading length (VSL), the variable chip rate (VCR), and the variable chip rate with frequency shift (VCRFS) formats. Their performance is compared for the case that a linear one-shot multiuser receiver is employed. It is also shown that detection of the users transmitting at the higher rate requires a periodically time-varying processing of the observables. Moreover, the problem of blind adaptive receiver implementation is studied, and a cyclic blind recursive-least-squares (RLS) algorithm is provided which is capable of converging to the periodically time-varying high-rate users detection structure.**

Numerical results show that the proposed receivers are near–far resistant, and that the VCRFS access technique achieves the best performance. Finally, as to the adaptive blind receiver implementation, computer simulations have revealed that the cyclic RLS algorithm for blind adaptive high-rate users demodulation outperforms the conventional RLS algorithm in most cases of primary importance.

***Index Terms*—DS-CDMA, multirate systems, multiple access interference, multiuser detection, recursive-least-squares.**

I. INTRODUCTION

A SUBSTANTIAL amount of work is available in the literature about multiuser detection for direct-sequence (DS) code division multiple access (CDMA) communication systems (see [1] and references therein). The main result of such works is that multiple access interference (MAI), when explicitly accounted for at the design stage, does not represent a heavily limiting factor, so it is possible to achieve satisfactory performance, even in a near–far scenario, at the price of a complexity increase in the receiver.

Based on this result, there has recently been a focus on the design of blind adaptive multiuser detectors which, while maintaining the MAI rejection capabilities of their nonadaptive counterparts, do not require explicit knowledge of the MAI structure, i.e., the number of interfering users, their relative delays, and their spreading sequences [2]–[4]. These blind adaptive detection structures have been shown to perform very well, and turn out to be very attractive when considering adoption of multiuser detection strategies in portable handset terminals.

However, most parts of the existing literature on DS/CDMA share one common hypothesis, i.e., that all of the users simultaneously accessing the channel transmit their information sequences with one and the same data rate. On the other hand, future multimedia wireless communication networks will have to accommodate a heterogeneous variety of information streams, including, beyond voice, packet data, low-resolution video, multimedia electronic mail, etc.; these information streams possess inherently different data rates, and are to be transmitted with different quality of service (QoS) requirements. Additionally, many of the existing CDMA-based standards for the forthcoming third-generation wireless networks, for instance, the wideband CDMA (WCDMA) [5], support the provision of multirate traffic with different QoSs. It is thus of primary interest to investigate possible modulation formats able to accommodate information streams with different data rates over a CDMA network, as well as to devise proper detection structures and blind adaptive algorithms taking into account the multirate nature of the received signal.

So far, two types of multirate access schemes have been mostly considered, namely the multicode (MC) and the variable spreading length (VSL) ones. The MC method [6] amounts to considering a single rate system, and to assigning to each user a number of spreading sequences tied to its bit rate; otherwise stated, high-rate users are able to transmit, in just one signaling interval of the single-rate system, several bits in parallel, and each high-rate user is thus converted in two or more virtual users transmitting at a lower rate. In the VSL access method, instead, all the users are characterized by the same chip rate (so as to maintain the same bandwidth requirements for each user) and signals with different data rates are accommodated by assigning spreading sequences with different lengths. Due to the serial/parallel and parallel/serial conversions, executed at the modulation and demodulation stages, respectively, the MC strategy is inherently affected by a decision lag, and has been shown to achieve poorer performance than the VSL access scheme [7], [8]. For the VSL access scheme, the decorrelating (zero-forcing) detector [9], [10], the minimum mean square error (MMSE) detector [11], [12] and a decision-feedback decorrelating detector [13] have been derived and analyzed under the assumption that the CDMA system is synchronous.

In this paper, we focus on an *asynchronous* dual-rate DS/CDMA network and deal with the issue of blind adaptive linear multiuser detection. We consider three possible access schemes, namely the VSL method, the variable chip rate (VCR) technique, which has been considered also in [14], and the

Manuscript received May 17, 1999; revised January 7, 2000 and May 29, 2000. This paper was presented in part at the 9th International Symposium on Personal Indoor and Mobile Radio Communications (PIMRC'98), Boston, MA, September 1998 and at the 1999 IEEE Global Communications Conference (GLOBECOM'99), Rio de Janeiro, Brazil, December 1999.

S. Buzzi and M. Lops are with DAEIMI, Universitá degli Studi di Cassino, Italy (e-mail: buzzi@unicas.it; lops@unicas.it).

A. M. Tulino is with DIET, Università degli Studi di Napoli "Federico II," Naples, Italy (e-mail: tulino@diesun.die.unina.it).

Publisher Item Identifier S 0733-8716(01)00830-7.

variable chip rate frequency shifted (VCRFS) method [15]. Overall, the main contributions of this paper may be summarized as follows: 1) to carry out a comparative performance assessment for the three considered access schemes, and in particular to show that the VCRFS, which amounts to adopting complex signatures for the low-rate users, outperforms the other two formats; 2) starting from the now well-established result that detection of the high-rate users requires periodically time-varying processing, to show how an adaptive (cyclic)recursive-least-squares (RLS)-based receiver can be designed, taking into account such a periodicity; 3) to present a sensitivity study, aimed at comparing the new cyclic RLS algorithm to the classical time-invariant RLS procedure, so as to emphasize the respective advantages and drawbacks. Finally, a nice byproduct of this paper is also an analysis of the convergence properties of the cyclic RLS, which can be obtained by generalizing similar results holding for time-invariant algorithms.

II. The Multirate Access Schemes

Let us consider an asynchronous dual-rate DS/CDMA network wherein users are allowed to transmit with one out of two different data rates. Even though all of the results presented throughout the paper can be easily generalized to a multirate system, in this paper we consider a system with only two possible data rates. In the following, all the active users will be grouped in two categories: those transmitting with the larger of the two available data rates will be referred to as *high-rate* users, while the remaining users (transmitting with the slower data rate) will be referred to as *low-rate* users.

Assuming that the signaling time of the low-rate users, $T_b^{(l)}$ say, and that of the high-rate users, $T_b^{(h)}$ say, are related as $T_b^{(l)} = LT_b^{(h)}$,[1] with L an integer positive number, and denoting by $K^{(h)}$ and $K^{(l)}$ the number of high-rate and low-rate active users, respectively, the complex envelope of the received waveform, $r(t)$ say, can be written as

$$r(t) = \sum_{m=-\infty}^{+\infty} \Bigg[\sum_{k=0}^{K^{(h)}-1} A_k^{(h)} e^{j\phi_k^{(h)}} b_k^{(h)}(m) s_k^{(h)}\left(t-\tau_k^{(h)}-mT_b^{(h)}\right) + \sum_{k=0}^{K^{(l)}-1} A_k^{(l)} e^{j\phi_k^{(l)}} b_k^{(l)}(m) s_k^{(l)} \times \left(t-\tau_k^{(l)}-mT_b^{(l)}\right) \Bigg] + w(t). \quad (1)$$

In (1), the superscripts (l) and (h) refer to the low-rate and high-rate users, respectively; $A_k^{(\cdot)} e^{j\phi_k^{(\cdot)}}$ represents a complex gain accounting for the propagation effects on the signal from the generic user, $\tau_k^{(\cdot)} \in [0, T_b^{(\cdot)}]$ and $s_k^{(\cdot)}(\cdot)$ are the delay and the signature waveform assigned to the generic kth user, respectively, while $\{b_k^{(h)}(\cdot)\}_{k=0}^{K^{(h)}-1}$ and $\{b_k^{(l)}(\cdot)\}_{k=0}^{K^{(l)}-1}$ represent the bit information streams, modeled as sequences of independent binary variates taking on values in the set $\{+1, -1\}$. Finally, $w(t)$ is the baseband equivalent of the thermal noise, modeled as a sample function from a zero-mean, white, complex Gaussian random process with power spectral density $2\mathcal{N}_0$.

[1]Such an assumption is made for sake of simplicity, but can be easily removed with minor modifications in subsequent derivations.

In the VSL access method, both high-rate and low-rate users share the same chip rate, whence users with different data rates are assigned spreading sequences with variable length. Accordingly, for the VSL system we have

$$\begin{aligned} s_k^{(l)}(t) &= \sum_{n=0}^{N^{(l)}-1} c_{n,k}^{(l)} u_{T_c^{(l)}}\left(t-nT_c^{(l)}\right) \\ s_k^{(h)}(t) &= \sum_{n=0}^{N^{(h)}-1} c_{n,k}^{(h)} u_{T_c^{(h)}}\left(t-nT_c^{(h)}\right) \end{aligned} \quad (2)$$

where $u_{T_c^{(\cdot)}}(\cdot)$ is a unit-height rectangular pulse supported on the interval $[0, T_c^{(\cdot)}]$, and $\{c_{n,k}^{(\cdot)}\}_{n=0}^{N^{(\cdot)}-1}$ is the spreading sequence assigned to the kth user.[2] Finally, in (2), $T_c^{(l)} = T_c^{(h)}$ is the common chip-interval and $N^{(l)} = LN^{(h)}$.

Beyond the VSL, in this paper we consider two additional access schemes. The first one, which will be referred to as variable chip rate (VCR), amounts to considering spreading sequences with the same length and different chip rates, i.e., we let $N^{(l)} = N^{(h)}$ and $T_c^{(l)} = LT_c^{(h)}$. Notice that with such a choice, the low-rate users occupy a bandwidth smaller than that occupied by the high-rate users; as a consequence, it is possible to allocate the carrier frequency of the signals from the low-rate users at some distance from the carrier frequency of the signals from the high-rate users, so as to reduce mutual interference between high-rate and low-rate users. This idea thus leads to the VCRFS access method, in which the spreading sequence for the kth low-rate user is given by

$$s_k^{(l)}(t) = \left(\sum_{n=0}^{N^{(l)}-1} c_{n,k}^{(l)} u_{T_c^{(l)}}\left(t-nT_c^{(l)}\right) \right) e^{j2\pi f^{(l)} t} \quad (3)$$

where, again, $N^{(l)} = N^{(h)}$ and $T_c^{(l)} = LT_c^{(h)}$. The parameter $f^{(l)}$ is the frequency offset between the carrier frequencies of the low-rate and high-rate CDMA signals. It is understood that, as $f^{(l)}$ increases, the mutual interference between the high-rate and low-rate users vanishes; on the other hand, $f^{(l)}$ cannot be chosen arbitrarily large, as it influences the bandwidth requirements of the overall multirate system. Here, we let $f^{(l)} = (1/T_c^{(h)}) - (1/T_c^{(l)})$, so that the main lobe of the Fourier transform of the low-rate users signature waveforms is entirely contained in the frequency range occupied by the main lobe of the Fourier transform of the high-rate users signature waveforms.

Let us assume, without any loss of generality, that the low-rate user "0" is the user of interest, that $\tau_0^{(l)} = 0$, and that we are interested in decoding the bit $b_0^{(l)}(p)$. To this end, we consider as

[2]Notice that we are here focusing on *periodic* spreading sequences; indeed, even though aperiodic (i.e., longer that one bit interval) sequences have been considered in current third-generation standards, periodic sequences are of great interest as they enable adoption of standard adaptive filtering techniques, and are also optionally supported in the uplink of the WCDMA standard proposal [5], as well as in the downlink of some proposals for third-generation satellite CDMA networks [16].

processing window the interval $\mathcal{I}_p^{(l)} = [(p-V)T_b^{(l)}, (p+V+1)T_b^{(l)}]$, namely we focus on the received signal as observed in the $(2V+1)$ signaling intervals including and surrounding the pth interval [17]. Since it is desirable to deal with a discrete-time signal, we are to project the signal, as observed in the interval $\mathcal{I}_p^{(l)}$, along a proper orthonormal set. Here, we adopt the following orthonormal system [15]:

$$\mathcal{B}_M^{(l)}(p) = \left\{ \frac{1}{\sqrt{T_{OS}}} \times u_{T_{OS}}\left(t - iT_{OS} - pT_b^{(l)}\right) e^{j2\pi f_s t} \right\}_{i=-N^{(h)}LMV}^{N^{(h)}LM(V+1)-1}$$

wherein $f_s = 0$ for the VSL or VCR access scheme, and $f_s = f^{(l)}$ for the VCRFS scheme, while $T_{OS} = T_c^{(h)}/M$ and M is an integer positive number. Notice that, if $M = 1$ and the VSL scheme is in force, projection onto the above set coincides with plain chip-matched filtering and chip rate sampling, while letting $M > 1$ corresponds to oversampling the received waveform [18].

The $N^{(h)}LM(2V+1)$-dimensional vector, $\boldsymbol{r}^{(l)}(p)$ say, obtained upon projection of the received waveform (1) along $\mathcal{B}_M^{(l)}(p)$ can be written as

$$\boldsymbol{r}^{(l)}(p) = A_0^{(l)} e^{j\phi_0^{(l)}} b_0^{(l)}(p) \boldsymbol{s}_{00}^{(l)} + \boldsymbol{z}(p) + \boldsymbol{w}(p) \tag{4}$$

wherein the first term on the right-hand side of (4) represents the contribution from the bit $b_0^{(l)}(p)$ to be decoded, while the other terms represent the low-rate and high-rate MAI $(\boldsymbol{z}(p))$, and the thermal noise contribution, respectively.

Let us now specify the signal model for the detection of the high-rate users. Assuming that the high-rate user "0" is the user of interest, that $\tau_0^{(h)} = 0$, and that we are interested in decoding the bit $b_0^{(h)}(p)$, we consider as processing window the interval $\mathcal{I}_p^{(h)} = [(p-V)T_b^{(h)}, (p+V+1)T_b^{(h)}]$. Considerations similar to those already illustrated suggest projecting the received waveform onto the following orthonormal set:

$$\mathcal{B}_M^{(h)}(p) = \left\{ \frac{1}{\sqrt{T_{OS}}} u_{T_{OS}}\left(t - iT_{OS} - pT_b^{(h)}\right) \right\}_{i=-N^{(h)}MV}^{N^{(h)}M(V+1)-1} \tag{5}$$

wherein $T_{OS} = T_c^{(h)}/M$ and M is an integer positive number. Such a set can be now adopted for any of the considered access techniques. We thus obtain the following $N^{(h)}M(2V+1)$-dimensional discrete-time sequence:

$$\boldsymbol{r}^{(h)}(p) = A_0^{(h)} e^{j\phi_0^{(h)}} b_0^{(h)}(p) \boldsymbol{s}_{00}^{(h)} + \boldsymbol{z}(p) + \boldsymbol{w}(p) \tag{6}$$

wherein, again, the first term on the right-hand side represents the contribution from the user of interest, while the other two terms represent the MAI and the thermal noise contributions. With a slight notational abuse, we still denote by $\boldsymbol{z}(p)$ and $\boldsymbol{w}(p)$ these terms, even though their expressions do not obviously coincide with those in (4).

It is worth noticing that in (6) an unitary increment in the index p corresponds to a temporal shift of $T_b^{(h)}$, which is a cyclostationarity period for the high-rate signals but *not* for the low-rate users. As a consequence, since $T_b^{(h)} = T_b^{(l)}/L$, it can be easily shown that the interference covariance matrix $\boldsymbol{R}_{\boldsymbol{zz}}(p) = E[\boldsymbol{z}(p)\boldsymbol{z}^H(p)]$ is periodically time-varying with period L, and so is its range span [15]: in other words, the situation here is akin to that outlined in [19] and [20] where a single-rate CDMA system is affected by a digital narrowband interfering signal and the ratio between the respective signaling intervals is a rational number.

III. Linear Multiuser Detection in Dual-Rate Networks

To begin with, let us consider the problem of decoding the bit $b_0^{(l)}(p)$ based on the processing of the $LN^{(h)}M(2V+1)$-dimensional vector $\boldsymbol{r}^{(l)}(p)$. To this end, we resort to a linear one-shot detection rule, i.e.,

$$\hat{b}_0^{(l)}(p) = \operatorname{sgn}\left\{ \mathbb{R}\left[\left(\boldsymbol{m}_0^{(l)}(p)\right)^H \boldsymbol{r}^{(l)}(p) \right] \right\} \tag{7}$$

wherein $\operatorname{sgn}(\cdot)$ is the signum function, $(\cdot)^H$ denotes conjugate transpose, and $\mathbb{R}(\cdot)$ denotes real part. As to $\boldsymbol{m}_0^{(l)}(p)$, it is an $LN^{(h)}M(2V+1)$-dimensional vector representing the receiver operation. The most popular linear receivers are the MMSE detector, which corresponds to

$$\boldsymbol{m}_0^{(l)} = A_0^{(l)} e^{j\phi_0^{(l)}} \left(\boldsymbol{R}_{\boldsymbol{r}^{(l)}\boldsymbol{r}^{(l)}}\right)^{-1} \boldsymbol{s}_{00}^{(l)} \tag{8}$$

and the decorrelating detector which, instead, is given by

$$\boldsymbol{m}_0^{(l)} = \left(\boldsymbol{R}_{\boldsymbol{h}^{(l)}\boldsymbol{h}^{(l)}}\right)^{\dagger} e^{j\phi_0^{(l)}} \boldsymbol{s}_{00}^{(l)}. \tag{9}$$

In the above equations, the covariance matrices $\boldsymbol{R}_{\boldsymbol{r}^{(l)}\boldsymbol{r}^{(l)}}$ and $\boldsymbol{R}_{\boldsymbol{h}^{(l)}\boldsymbol{h}^{(l)}}$ are defined as

$$\begin{aligned} \boldsymbol{R}_{\boldsymbol{r}^{(l)}\boldsymbol{r}^{(l)}} &= E\left[\boldsymbol{r}^{(l)}(p) \left(\boldsymbol{r}^{(l)}(p)\right)^H \right], \\ \boldsymbol{R}_{\boldsymbol{h}^{(l)}\boldsymbol{h}^{(l)}} &= E\left[\left(\boldsymbol{r}^{(l)}(p) - \boldsymbol{w}(p)\right) \left(\boldsymbol{r}^{(l)}(p) - \boldsymbol{w}(p)\right)^H \right]. \end{aligned} \tag{10}$$

$(\cdot)^{\dagger}$ denotes the Moore–Penrose generalized inverse [21], and the dependence of the filter $\boldsymbol{m}_0^{(l)}$ on the temporal index p has been dropped as not actually present. Notice that, if the vector $\boldsymbol{s}_{00}^{(l)}$ does not lie in the range span $\mathcal{R}(\boldsymbol{R}_{\boldsymbol{zz}})$ of the interference covariance matrix $\boldsymbol{R}_{\boldsymbol{zz}} = E[\boldsymbol{z}(p)\boldsymbol{z}^H(p)]$, then the interference contribution at the output of the decorrelating receiver is totally nullified as the filter (9) performs a projection of the observables onto the orthogonal complement of the interference subspace $\mathcal{R}(\boldsymbol{R}_{\boldsymbol{zz}})$.

As regards detection of the high-rate users, once again we consider the following linear decision rule:

$$\hat{b}_0^{(h)}(p) = \operatorname{sgn}\left\{ \mathbb{R}\left[\left(\boldsymbol{m}_0^{(h)}(p)\right)^H \boldsymbol{r}^{(h)}(p) \right] \right\} \tag{11}$$

with $\boldsymbol{m}_0^{(h)}(p)$ a $N^{(h)}M(2V+1)$-dimensional vector expressed as

$$\boldsymbol{m}_0^{(h)}(p) = A_0^{(h)} e^{j\phi_0^{(h)}} \left(\boldsymbol{R}_{\boldsymbol{r}^{(h)}\boldsymbol{r}^{(h)}}(p)\right)^{-1} \boldsymbol{s}_{00}^{(h)} \tag{12}$$

for the MMSE detector, and

$$\boldsymbol{m}_0^{(h)}(p) = \left(\boldsymbol{R}_{\boldsymbol{h}^{(h)}\boldsymbol{h}^{(h)}}(p)\right)^{\dagger} e^{j\phi_0^{(h)}} \boldsymbol{s}_{00}^{(h)} \tag{13}$$

for the decorrelating detector, respectively. Of course, in (12) and (13) the matrices $\boldsymbol{R}_{\boldsymbol{r}^{(h)}\boldsymbol{r}^{(h)}}(p)$ and $\boldsymbol{R}_{\boldsymbol{h}^{(h)}\boldsymbol{h}^{(h)}}(p)$ are the covariance matrix of the vectors $\boldsymbol{r}^{(h)}(p)$ and $\boldsymbol{h}^{(h)}(p) = \boldsymbol{r}^{(h)}(p) - \boldsymbol{w}(p)$.

Notice that, even though in (12) and (13) the filter $\boldsymbol{m}_0^{(h)}(\cdot)$ is time-varying, it is actually a periodically time-varying quantity with period L, implying that receiver implementation does not require an *on-line* (heavy) computation of the filter at any bit interval: the high-rate receiver is just defined by L coefficient sets, $\{\boldsymbol{m}_0^{(h)}(p)\}_{p=0}^{L-1}$, to be cyclically employed in order to decode the information stream from the high-rate user "0" [15].

A. Numerical Results

In this subsection, we present some sample plots illustrating the performance of the linear multiuser detectors in a multirate environment. To this aim, we consider a dual-rate asynchronous DS/CDMA system with $L = 2$, namely one of the two available data rates is twice as large as the other. Gold codes have been adopted as signature sequences, with processing gain $N^{(h)} = 31$. For the VSL access technique, the low-rate spreading sequences of length $N^{(l)} = LN^{(h)} = 62$ have been built by replicating Gold codes of length 31. Moreover, the following plots are the result of an average over 100 randomly generated realizations of the CDMA signals delays.

First of all, let us carry out a comparative analysis of the performance of the three considered access schemes. In Figs. 1 and 2, the bit error rate (BER) of the MMSE and decorrelating detectors for the high-rate and low-rate users signals are presented, respectively, versus the received energy contrast per bit, defined as

$$\frac{\mathcal{E}_b^{(\cdot)}}{\mathcal{N}_0} = \frac{\left(A_0^{(\cdot)}\right)^2 T_b^{(\cdot)}}{\mathcal{N}_0}$$

for $V = 0$ (i.e., the processing window equals the signaling time), an oversampling ratio $M = 3$, and for all of the three considered access schemes. The users number has been set equal to 20, assuming $K^{(h)} = K^{(l)} = 10$. For the MMSE detector, it has been assumed that all of the interfering users possess an amplitude which is five dB greater than that of the user of interest; conversely, the interfering users amplitudes are not a relevant parameter for the BER of the zero-forcing detector. As expected, and in keeping with well-known results for single-rate systems, the curves show that for any of the three access techniques, the MMSE detector outperforms the decorrelating detector. Additionally, it is seen that, for the high-rate users, the VCR access technique performs better than the VSL while, on the contrary, for the low-rate users, the VCR is worse than the VSL. These results can be easily justified. Indeed, in the VCR technique, the low-rate users are assigned a chip interval which is twice as large as that of the high-rate users; the low-rate users are thus a minor source of interference for the high-rate ones, in that they occupy half the bandwidth required for the VSL method, and have higher degree of coherence. On the other hand, under the VCR technique, the low-rate users are assigned a spreading sequence with half the processing gain as compared to the VSL, and are affected by a *wideband* disturbance (i.e., the high-rate CDMA system whose chip rate is twice that of the low-rate users). The VCRFS access technique, instead, is seen to outperform the other two access schemes for both the low-rate and high-rate signals. This result confirms the previously anticipated intuition that, due to the low-pass nature of the waveforms $u_{T_c^{(\cdot)}}(\cdot)$, allocating the carrier frequency of the low-rate signals at some distance from that of the high-rate system results in reduced mutual interference between the two systems, and, eventually, in better performance.

In Fig. 3, the effects on the system BER of oversampling and of the processing window enlargement is investigated for the high-rate users. Precisely, we have considered the MMSE detector and the VCRFS access technique, which have been shown to yield the best performance; the number of users accessing simultaneously the channel is still 20. As expected, results show that both an enlargement of the processing window and an increase in the oversampling factor result in improved system performance.

Finally, similar conclusions can be drawn by inspecting Fig. 4, wherein the system near–far resistance, averaged over 100 randomly generated other-users delays, for the high-rate users, has been plotted, for several values of V and M and for the VCRFS access technique. The Abscissa represents the overall users number $K^{(h)} + K^{(l)}$: precisely, the even numbers refer to the case that the low-rate and high-rate users numbers are equal, i.e., $K^{(l)} = K^{(h)}$, while the odd numbers refer to the case in which the high-rate users are in excess by one on the low-rate users.

IV. Blind Adaptive MMSE Detection

In this section, we dwell on the exposition of an RLS-based algorithm for blind adaptive MMSE detection, wherein no prior knowledge on the interfering signals parameters is available to the receiver.

To this end, we recall that the linear MMSE multiuser detector may be implemented in a blind adaptive fashion by exploiting its equivalence with the minimum-output-energy (MOE) receiver [2], [23]. In particular, as regards decoding of the low-rate users, based on the observables $\boldsymbol{r}^{(l)}(1), \ldots, \boldsymbol{r}^{(l)}(n)$, a blind adaptive implementation of the (time-invariant) receiver (8) may be obtained by solving the following exponentially windowed constrained minimization problem:

$$\begin{cases} \displaystyle\sum_{i=1}^{n} \lambda^{n-i} \left| \left(\hat{\boldsymbol{m}}_0^{(l)}(n)\right)^H \boldsymbol{r}^{(l)}(i) \right|^2 = \min \\ \left(\hat{\boldsymbol{m}}_0^{(l)}(n)\right)^H \boldsymbol{s}_{00}^{(l)} = 1 \end{cases} \tag{14}$$

wherein $\hat{\boldsymbol{m}}_0^{(l)}(n)$ is the estimate, available at epoch n, of the true solution $\boldsymbol{m}_0^{(l)}$ specified in (8), and λ, usually referred to as "forgetting factor," is a scalar constant slightly smaller than unity which ensures the tracking capability of the solution. The solution to the problem (14) may be iteratively computed by resorting to well-known procedures, for instance, those developed in [3] and [23].

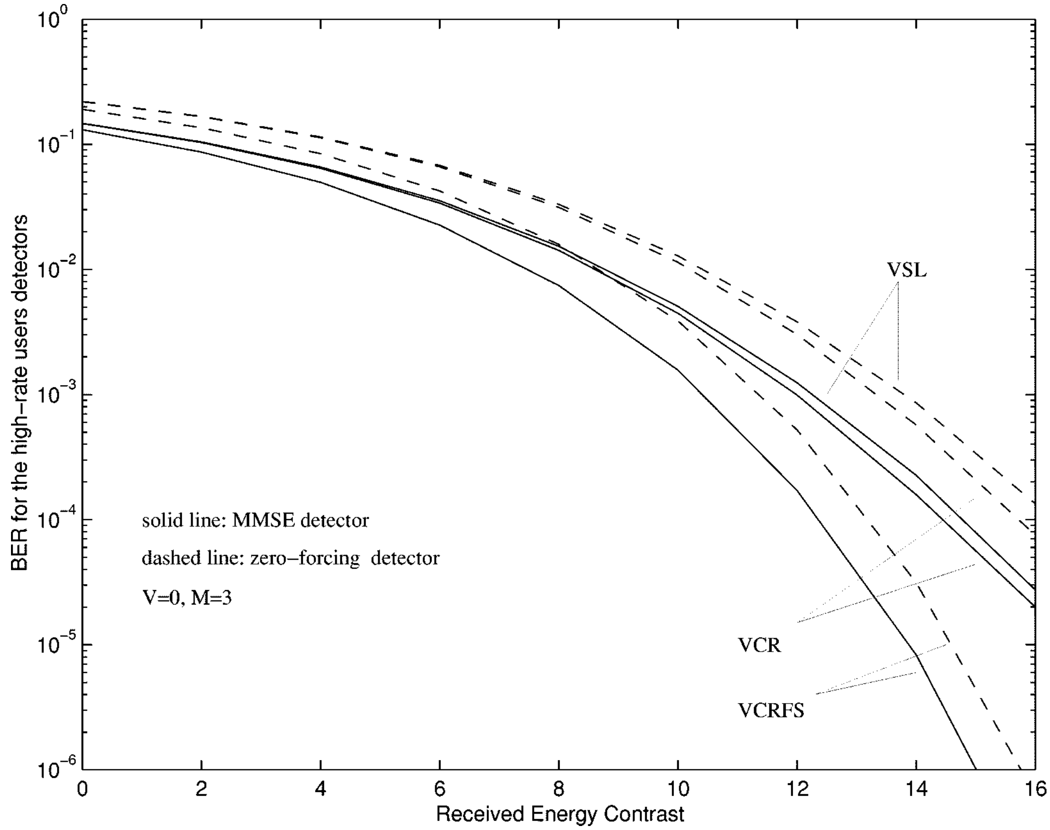

Fig. 1. BER for the MMSE and zero-forcing detector for the high-rate users.

Let us instead consider the problem of blind adaptive high-rate users detection. In this situation, indeed, the detection rule is periodically time-varying with period L, whence conventional adaptive methods, which assume that the solution to be tracked is stationary or slowly varying, are not suited for high-rate users detection, as they are not able to converge to a periodically time-varying receiving structure. Accordingly, in what follows, we propose a *cyclic* RLS algorithm, which enables blind adaptive implementation of the high-rate users detector.

A. Cyclic RLS Algorithm

In a periodically time-varying scenario, i.e., when a high-rate user is to be decoded, an *adaptive* RLS-based receiver is to track a periodical solution, which entails reformulation of the constrained minimization problem (14). Dropping, for notational simplicity, the superscript $(\cdot)^{(h)}$, we define by $\hat{\boldsymbol{m}}_0(n,i)$ the estimate of the periodically time-varying sequence $\boldsymbol{m}_0(i)$, available after observing the n vectors $\boldsymbol{r}(1),\ldots,\boldsymbol{r}(n)$. Such an estimate is subsequently employed to make the decision

$$\begin{aligned}\hat{b}_0(n) &= \operatorname{sgn}\left[\mathbb{R}\left\{\hat{\boldsymbol{m}}_0^H(n,n)\boldsymbol{r}(n)\right\}\right]\\ &= \operatorname{sgn}\left[\mathbb{R}\left\{\hat{\boldsymbol{m}}_0^H(n,n \bmod L)\boldsymbol{r}(n)\right\}\right] \qquad (15)\end{aligned}$$

where the equivalence between the last two terms of the above equation stems from the fact that the estimator $\hat{\boldsymbol{m}}_0(n,i)$ should be periodical in its second argument with period L. In order to determine the estimate $\hat{\boldsymbol{m}}_0(n,i)$, once again we resort to minimizing the exponentially weighted output energy. More precisely, a receiver adopting the estimate $\hat{\boldsymbol{m}}_0(n,i)$ in place of the true periodically time-varying vector sequence achieves an exponentially-weighted output energy

$$\begin{aligned}&\sum_{i=1}^{n}\lambda^{n-i}\left|\hat{\boldsymbol{m}}_0^H(n,i)\boldsymbol{r}(i)\right|^2\\ &\quad=\sum_{i=1}^{n}\lambda^{n-i}\left|\hat{\boldsymbol{m}}_0^H(n,i \bmod L)\boldsymbol{r}(i)\right|^2\end{aligned}$$

wherein, again, λ is the "forgetting factor." The optimum (in the MOE sense) estimator is, thus, the solution to the following constrained minimization problem

$$\begin{cases}\displaystyle\sum_{i=1}^{n}\lambda^{n-i}\left|\hat{\boldsymbol{m}}_0^H(n,i)\boldsymbol{r}(i)\right|^2=\min\\ \hat{\boldsymbol{m}}_0^H(n,i)\boldsymbol{s}_{00}=1 \qquad \forall\, i=1,\ldots,L.\end{cases} \qquad (16)$$

Deferring to the Appendix the mathematical details, if we define

$$\begin{aligned}\tilde{\boldsymbol{r}}(i) &= \left[\boldsymbol{r}^H(i),\boldsymbol{r}^H(i)\exp\left(j\frac{2\pi i}{L}\right),\right.\\ &\qquad \left.\ldots,\boldsymbol{r}^H(i)\exp\left(j\frac{2\pi(L-1)i}{L}\right)\right]^H\\ \tilde{\boldsymbol{R}}(n) &= \sum_{i=1}^{n}\lambda^{n-i}\tilde{\boldsymbol{r}}(i)\tilde{\boldsymbol{r}}^H(i) \qquad (17)\end{aligned}$$

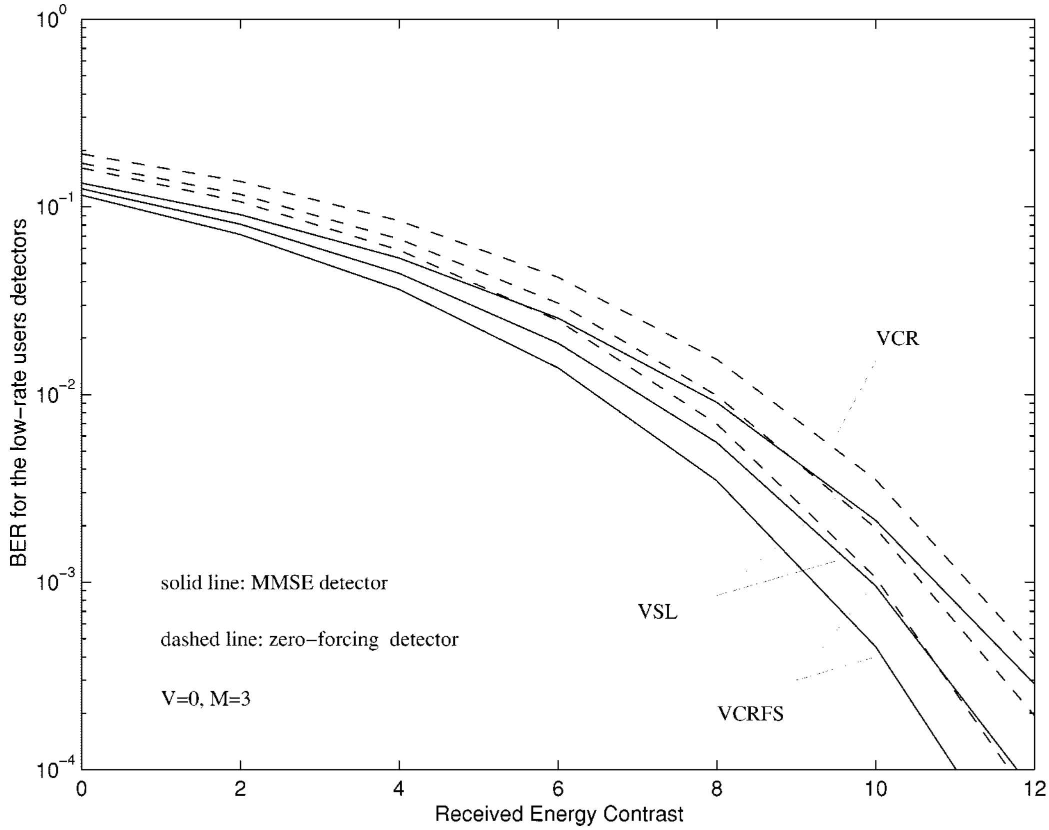

Fig. 2. BER for the MMSE and zero-forcing detector for the low-rate users.

then the solution to (16) may be obtained through the following recursive algorithm:

$$\begin{aligned}\tilde{\boldsymbol{k}}(n) &= \frac{\tilde{\boldsymbol{R}}^{-1}(n-1)\tilde{\boldsymbol{r}}(n)}{\lambda + \tilde{\boldsymbol{r}}^H(n)\tilde{\boldsymbol{R}}^{-1}(n-1)\tilde{\boldsymbol{r}}(n)}\\ \tilde{\boldsymbol{R}}^{-1}(n) &= \frac{1}{\lambda}\left(\tilde{\boldsymbol{R}}^{-1}(n-1) - \tilde{\boldsymbol{k}}(n)\tilde{\boldsymbol{r}}^H(n)\tilde{\boldsymbol{R}}^{-1}(n-1)\right)\\ \boldsymbol{H}(n,n) &= \boldsymbol{\Psi}(n)\tilde{\boldsymbol{R}}^{-1}(n)\\ &= \frac{1}{\lambda}\Big(\boldsymbol{\Psi}(1)\boldsymbol{H}(n-1,n-1)\\ &\qquad - \boldsymbol{\Psi}(1)\boldsymbol{H}(n-1,n-1)\tilde{\boldsymbol{r}}(n)\tilde{\boldsymbol{k}}^H(n)\Big)\\ \boldsymbol{g}(n,n) &= \boldsymbol{e}_2^H \otimes \boldsymbol{I}_{N^{(h)}M(2V+1)}\boldsymbol{H}(n,n)\tilde{\boldsymbol{S}}_0\boldsymbol{e}_1\\ \hat{\boldsymbol{m}}_0(n,n) &= \frac{\boldsymbol{g}(n,n)}{\left(\boldsymbol{s}_{00}^H\boldsymbol{g}(n,n)\right)}\end{aligned} \tag{18}$$

wherein $\otimes$ denotes Kronecker product [21], and we have let

$$\begin{aligned}\boldsymbol{\Psi}(n) =& \,\mathrm{Diag}\left(\left[1, \exp\left(j\frac{2\pi n}{L}\right), \exp\left(j\frac{2\pi 2n}{L}\right), \ldots,\right.\right.\\ &\left.\left.\exp\left(j^2\frac{\pi(L-1)n}{L}\right)\right]^T\right)\\ &\otimes \boldsymbol{I}_{N^{(h)}M(2V+1)}\\ \tilde{\boldsymbol{S}}_0 =& \,\boldsymbol{I}_L \otimes \boldsymbol{s}_{00} \quad \boldsymbol{e}_1 = [1, \underbrace{0, \ldots, 0}_{L-1}]^T\\ \boldsymbol{e}_2 =& \,[\underbrace{1, 1, \ldots, 1}_{L}]^T\end{aligned} \tag{19}$$

with $\boldsymbol{I}_L$ the identity matrix of order L. Some remarks about the proposed algorithm are now in order. First of all, notice that it may be implemented based on the knowledge of the signature waveform and of the timing of the user to be decoded, as well as of the high-rate signaling interval or, equivalently, of L. Moreover, $\tilde{\boldsymbol{R}}(n)$ is a square $LN^{(h)}M(2V+1)$-dimensional block-circulant matrix with the following structure:

$$\tilde{\boldsymbol{R}}(n) = \begin{pmatrix} \boldsymbol{R}^{(0)}(n) & \boldsymbol{R}^{(1)}(n) & \cdots & \boldsymbol{R}^{(L-1)}(n)\\ \boldsymbol{R}^{(L-1)}(n) & \boldsymbol{R}^{(0)}(n) & \cdots & \boldsymbol{R}^{(L-2)}(n)\\ \vdots & \cdots & \cdots & \vdots\\ \boldsymbol{R}^{(1)}(n) & \boldsymbol{R}^{(2)}(n) & \cdots & \boldsymbol{R}^{(0)}(n)\end{pmatrix} \tag{20}$$

where $\boldsymbol{R}^{(\ell)}(n) = \sum_{i=0}^{n}\boldsymbol{r}(i)\boldsymbol{r}^H(i)e^{j(2\pi i\ell/L)}$ is the exponentially weighted time-averaged counterpart of the *cyclic* correlation matrix with cycle frequency parameter (ℓ/L) [24]. As a consequence, based on the block-circulant nature of the involved matrices, it can be shown that the actual algorithm complexity is linear in L, i.e., $O(L(N^{(h)}M(2V+1))^2)$ complex multiplications are needed so as to update the filter $\boldsymbol{m}_0(n,n)$; thus the complexity is just L times larger than that of a conventional RLS algorithm [25]. Additionally, since the modified RLS algorithm processes the vector $\tilde{\boldsymbol{r}}(\cdot)$, it is easily seen that it may be implemented through the so-called FREquency-SHift (FRESH) realization [24, Ch. 12] as depicted in Fig. 5. The time-varying receiver may be realized through a time-invariant processing preceeded by a set of complex oscillators, keyed to the harmonical frequencies $\{q/L\}_{q=0}^{L-1}$; the time-varying part of

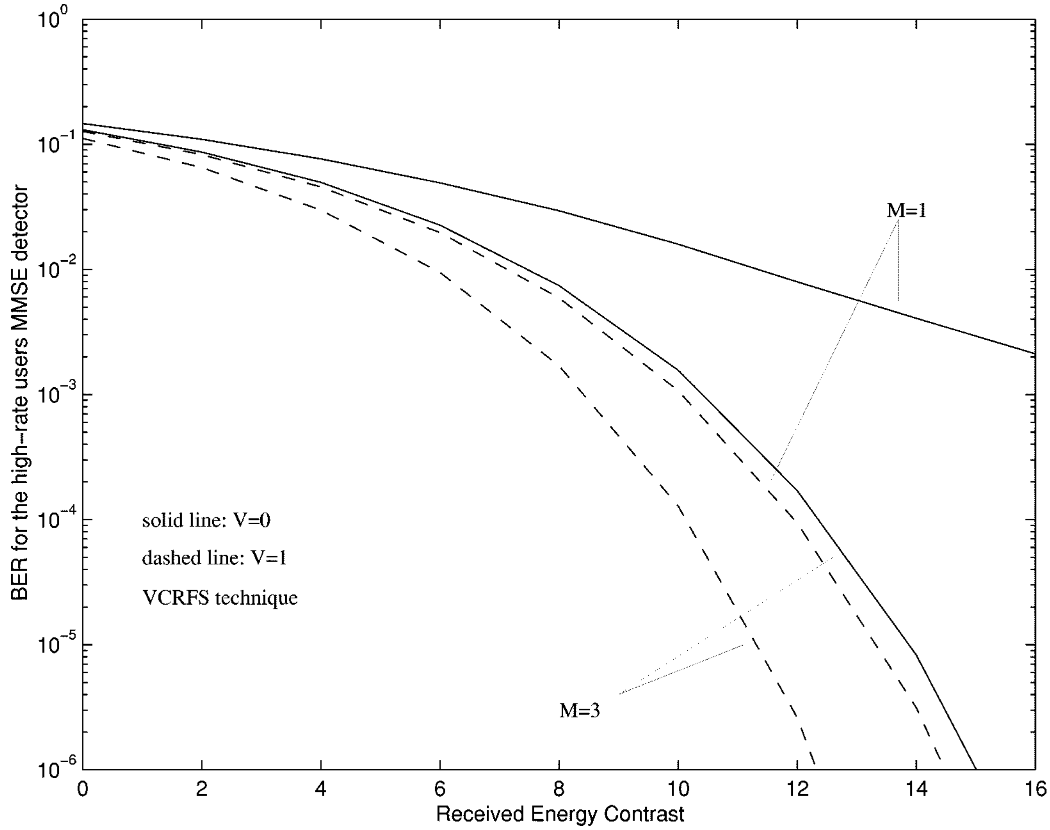

Fig. 3. BER for the high-rate signals MMSE detector with VCRFS access method.

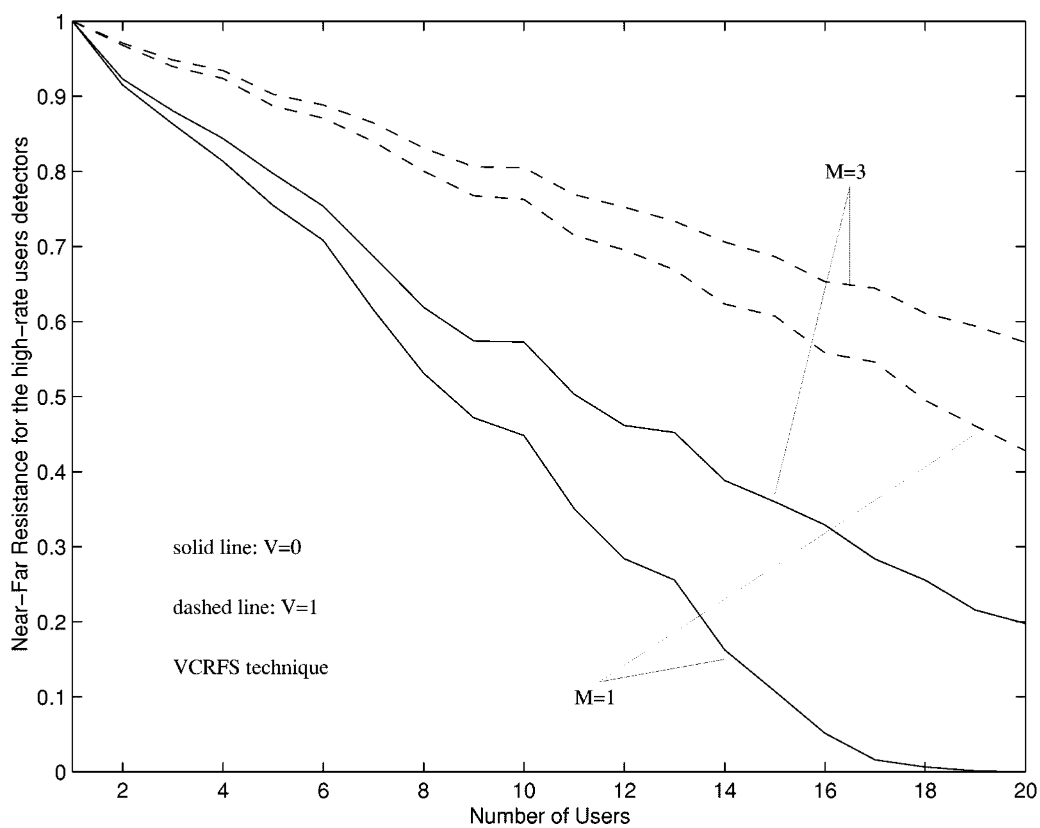

Fig. 4. Near–far resistance for the high-rate signals detectors with VCRFS access method.

the algorithm is thus confined to the bank of complex oscillators. The time-invariant processing amounts obviously to a multiplexer (MUX) and to a block implementing the RLS procedure (18) followed by the final decision circuits implementing the

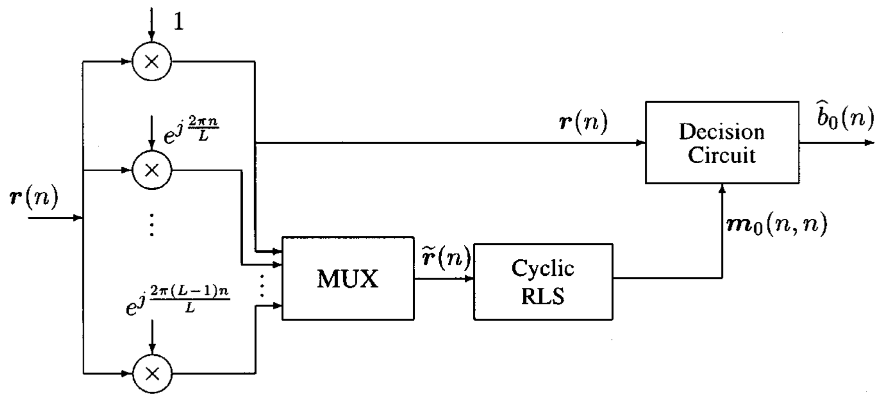

Fig. 5. FRESH implementation of the adaptive receiver.

decision rule $\hat{b}_0(n) = \text{sgn}\{\mathbb{R}(\boldsymbol{m}_0^H(n,n)\boldsymbol{r}(n))\}$. Finally, we notice that the FRESH solution presents a highly modular structure, which may turn out useful if the period L is very large: in this situation, indeed, one could resort to a FRESH structure containing a smaller number of complex oscillators. This choice would obviously lead to a suboptimal receiver, but would also permit to reduce the receiver complexity. Of course, the set of cyclic frequencies (to which the complex oscillators are to be keyed) should be chosen as a compromise between the conflicting requirements of achieving satisfactory performance and affordable receiver complexity. We do not dwell any longer on this point, which is the object of current investigation.

V. Analysis of the Blind Receiver

The proposed cyclic RLS-based adaptive procedure differs from the conventional RLS algorithm for two reasons: 1) it is blind, i.e., it does not require the periodical transmission of known training sequences; 2) for the case that an high-rate user is to be decoded it is *cyclic*, namely it is able to converge to a periodically time-varying receiving structure. As a consequence, well-known results on the convergence capabilities of the conventional RLS algorithm [25] do not apply to our context. Recently, a convergence analysis of the blind RLS algorithm has been presented in [3]; the results of this study obviously hold with no modification for the case of blind adaptive implementation of the low-rate users receiver *but* they are not valid for the companion case of blind adaptive high-rate users demodulation, since in this latter situation the receiver to be tracked is periodically time-varying.

In order to verify the effectiveness of the new algorithm, in what follows we focus on the case of periodically time-varying interference background. Unfortunately, a thorough convergence analysis of the algorithm (18) turned out to be unwieldly. As an indirect proof, and to establish somewhat reassuring results, in this paper we consider the case that no exponential windowing is adopted and the matrix $\tilde{\boldsymbol{R}}(n)$ is the sample covariance matrix, i.e.,

$$\tilde{\boldsymbol{R}}(n) = \frac{1}{n}\sum_{i=1}^{n}\tilde{\boldsymbol{r}}(i)\tilde{\boldsymbol{r}}^H(i). \tag{21}$$

Notice that this assumption just causes a more limited capability of tracking changes in the interference structure (i.e., for instance, the birth of new users or changes in their amplitudes), while having no effects on the steady-state performance, i.e., on its capability of converging, in a stationary environment (i.e., with no changes in the interference structure), to the true periodically time-varying solution.

Finally, we validate the effectiveness of the new algorithm (18) through some computer simulation results.

A. Convergence Analysis

Here, we show that the proposed cyclic blind algorithm with $\tilde{\boldsymbol{R}}(n)$ as in (21) converges almost surely (a.s.) and in the mean value to the true solution, while the blind algorithm in [3] is not able to converge to the periodically time-varying true solution.

To begin with, we notice that, under mild assumptions, the matrix (21) converges a.s. to the following matrix [26, Ch. 7, p. 275]:

$$\tilde{\boldsymbol{R}}(n) \overset{\text{a.s.}}{\to} \tilde{\boldsymbol{R}}_{\tilde{\boldsymbol{r}}\tilde{\boldsymbol{r}}} = \left\langle E\left[\tilde{\boldsymbol{r}}(i)\tilde{\boldsymbol{r}}^H(i)\right]\right\rangle \tag{22}$$

with $\langle\cdot\rangle$ denoting time-average. The matrix $\tilde{\boldsymbol{R}}_{\tilde{\boldsymbol{r}}\tilde{\boldsymbol{r}}}$ is a $LN^{(h)}M(2V+1)$-dimensional square block-circulant matrix, with a structure similar to that in (20), and whose generic ℓth block (with $\ell = 0,\ldots,L-1$) $\boldsymbol{R}^{(\ell)}$ coincides with the observables cyclic correlation matrix with cycle frequency parameter (ℓ/L) [24]. Since, from (18) we have

$$\begin{aligned}\hat{\boldsymbol{m}}_0(n,n) &= \frac{\boldsymbol{g}(n,n)}{\left(\boldsymbol{s}_{00}^H\boldsymbol{g}(n,n)\right)}\\ &= \frac{\left(\boldsymbol{e}_2^H \otimes \boldsymbol{I}_{N^{(h)}M(2V+1)}\right)\boldsymbol{\Psi}(n)\tilde{\boldsymbol{R}}^{-1}(n)\tilde{\boldsymbol{S}}_0\boldsymbol{e}_1}{\left(\boldsymbol{s}_{00}^H\left(\boldsymbol{e}_2^H \otimes \boldsymbol{I}_{N^{(h)}M(2V+1)}\right)\boldsymbol{\Psi}(n)\tilde{\boldsymbol{R}}^{-1}(n)\tilde{\boldsymbol{S}}_0\boldsymbol{e}_1\right)}\end{aligned} \tag{23}$$

following the same steps as in the Appendix, it can be shown that, skipping irrelevant positive proportionality factors, $\hat{\boldsymbol{m}}_0(n,n)$ converges a.s. to the true solution (12).

Since the modulus of each entry of the vector $\hat{\boldsymbol{m}}_0(n,n)$ is uniformly integrable (with respect to the probability measure),

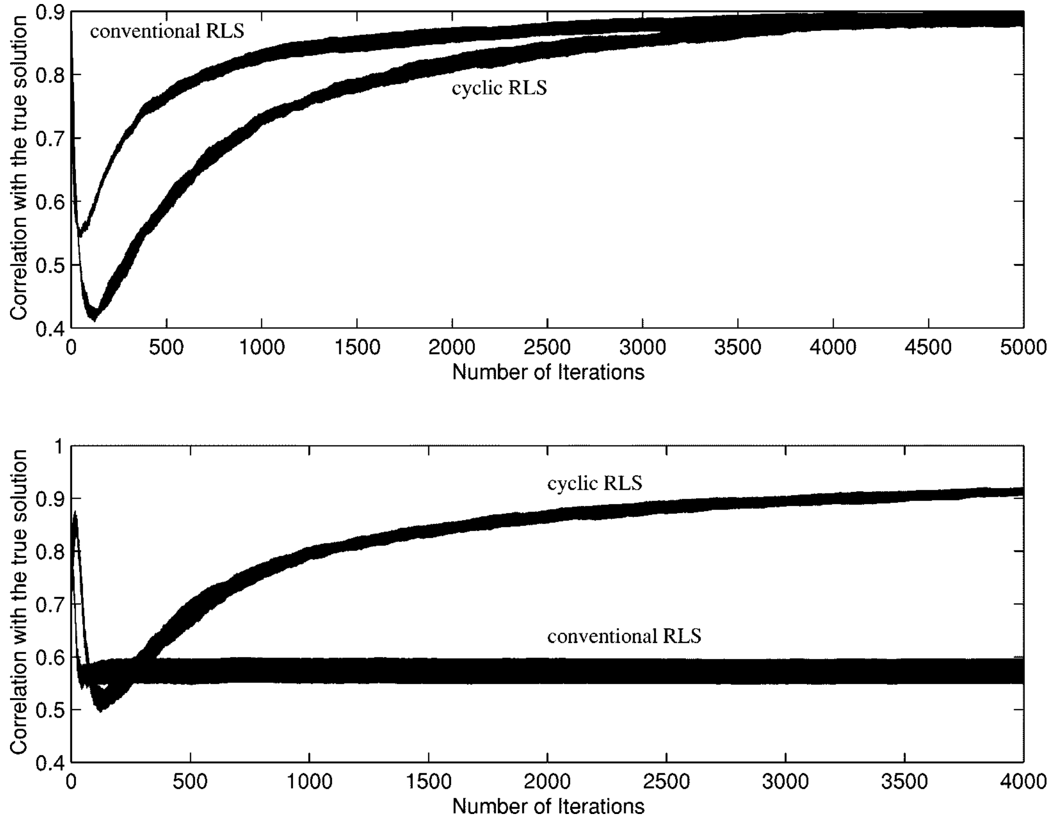

Fig. 6. Convergence dynamics of the cyclic and of the conventional blind RLS algorithms. System parameters: $K^{(h)} = 5$; $K^{(l)} = 12$; the upper plot refers to a power-controlled scenario, while in the lower plot the low-rate users amplitudes are 20 dB stronger than the high-rate users' amplitudes.

it follows [26, p. 297] that $\hat{\boldsymbol{m}}_0(n,n)$ converges in the mean value to the true solution.

Let us now consider the classical blind algorithm in [3]. Since, again, no exponential windowing is adopted, the said algorithm operates on the following sample covariance matrix:

$$\boldsymbol{R}(n) = \frac{1}{n}\sum_{i=1}^{n} \boldsymbol{r}(i)\boldsymbol{r}^H(i). \tag{24}$$

Under these circumstances, it is easy to show that, for increasing n, we have

$$\boldsymbol{R}(n) \xrightarrow{\text{a.s.}} \frac{1}{L}\sum_{p=0}^{L-1} \boldsymbol{R}_{\boldsymbol{r}^{(h)}\boldsymbol{r}^{(h)}}(p). \tag{25}$$

Otherwise stated, the matrix $\boldsymbol{R}(n)$ converges to the time-average of the statistical covariance matrices $\boldsymbol{R}_{\boldsymbol{r}^{(h)}\boldsymbol{r}^{(h)}}(p)$, with $p = 0, \ldots, L-1$. Since this limit is actually time-invariant, it is evident that the blind algorithm in [3] cannot converge to a periodically time-varying solution.

B. Simulation Examples

Once again, we have adopted Gold codes as spreading sequences, with processing gain $N^{(h)} = 31$; we have considered the VCRFS access technique, and we have set $L = 3$, i.e., the secondary CDMA network transmits at a rate three times slower than the primary network. In order to lower the simulation time we have considered a synchronous system, so as to skip the average with respect to the random delays. This assumption, however, as explained, for instance, in [2] and [3], does not imply any loss of generality. The forgetting factor λ has been set equal to 0.9995.

Since the convergence capabilities of the "time-invariant" blind RLS algorithm have been already illustrated in [3], we dwell here on the performance of the cyclic algorithm, i.e., we consider the problem of blind adaptive high-rate users demodulation. First of all, let us focus on the convergence dynamics of the algorithm. In Fig. 6, we have represented the correlation coefficient between the estimated filter $\hat{\boldsymbol{m}}_0(n,n)$ and the "true" filter $\boldsymbol{m}_0^{(h)}(n)$, whose expression is given by (12), versus the number of iterations. The plots are the result of an average over 100 random independent runs. The upper curve refers to a scenario with $K^{(h)} = 5$ and $K^{(l)} = 12$; all of the signals have the same amplitude (i.e., perfect power-control is assumed) and the average received energy contrast is 13 dB. The lower curve, instead, is similar to the former one, except for the fact that the low-rate users amplitudes are assumed to be 20 dB stronger than the high-rate amplitudes. It is seen that in the upper curve the cyclic algorithm and the conventional blind RLS (i.e., the one reported in [3]) achieve the same asymptotic value, *but* the convergence time of the cyclic algorithm is noticeably larger than that of the conventional one. In the lower curve, instead, the cyclic RLS algorithm largely outperforms the conventional one. Such a behavior is easily justified. Indeed, the need for a periodically time-varying detection rule is due to the presence of the low-rate users: in a perfectly power-controlled situation,

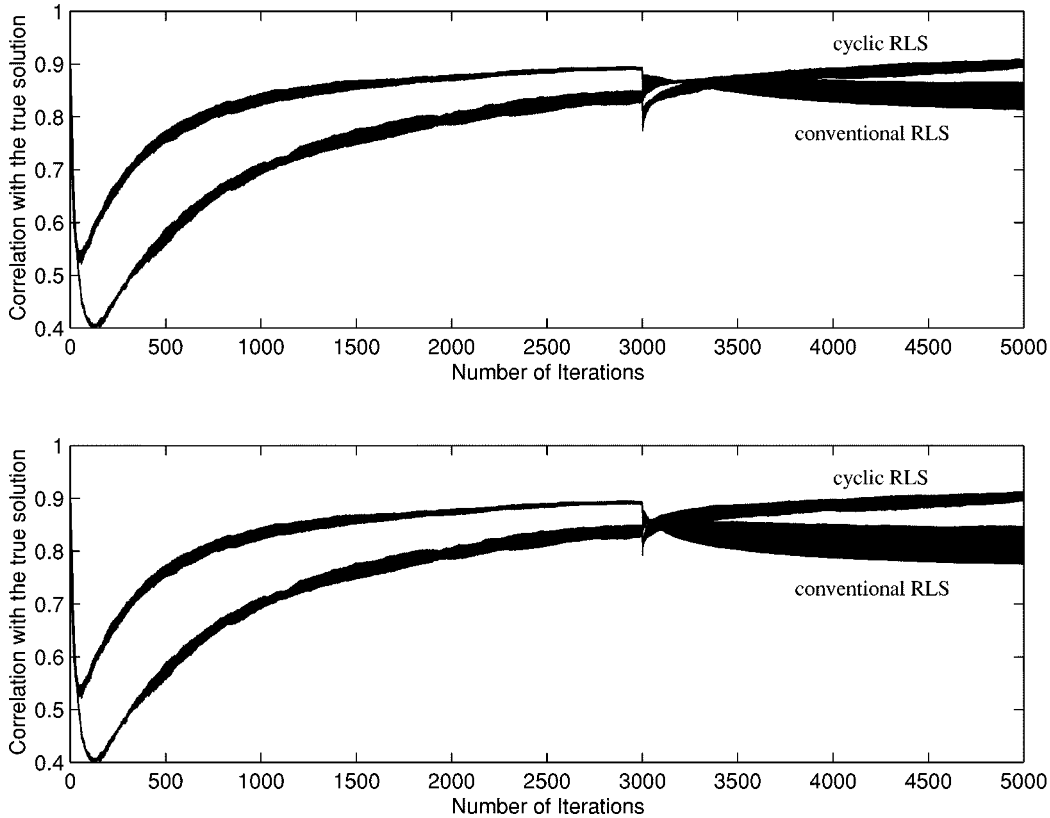

Fig. 7. Tracking capabilities of the cyclic and of the conventional blind RLS algorithms. Before epoch 3000, there are five high-rate users and nine low-rate users; at epoch 3000, 4 new low-rate users enter the channel. In the upper (lower) plot, the new users have 10-dB (20-dB) power advantage on the high-rate users.

the time-variations of the interference covariance matrix $\boldsymbol{R}_{\boldsymbol{zz}}(\cdot)$ are not very strong, whence the conventional RLS algorithm (which is suited for the tracking of a time-invariant, or slowly time-varying, interference covariance matrix) achieves satisfactory performance. Likewise, the cyclic algorithm achieves good performance as well, *but* converges more slowly due to the fact that its input vector $\tilde{\boldsymbol{r}}(\cdot)$ has a dimensionality L times larger than the dimensionality of the vector $\boldsymbol{r}(\cdot)$ which is processed by the conventional algorithm. In the lower curve, instead, the severe near–far scenario emphasizes the periodicity of the matrix $\boldsymbol{R}_{\boldsymbol{zz}}(\cdot)$, and so the conventional RLS algorithm is not able to track its variations. The cyclic algorithm, on the contrary, achieves very satisfactory performance and enables blind adaptive high-rate users demodulation. Other simulations, whose results are not shown here for sake of brevity, have revealed that the conventional algorithm performs poorer and poorer as the users number increases, even if perfect power control is assured; the cyclic algorithm, instead, is quite insensitive to the network load.

Let us now concentrate on the tracking capabilities of the algorithm. In Fig. 7, we have again represented the correlation coefficient between the estimated filter and the true solution (12). The upper curve initially refers to a scenario with $K^{(h)} = 5$ and $K^{(l)} = 9$; all of the signals have the same amplitude (i.e., perfect power-control is assumed) and the average received energy contrast is 13 dB; at epoch 3000, four low-rate users with an amplitude ten dB larger than that of the other signals enter the channel. The lower curve, instead, differs from the upper one as the nine low-rate users have an amplitude which is ten dB larger than that of the high-rate signals, while the four low-rate users entering the channel at epoch 3000 have an amplitude 20 dB stronger than that of the high-rate signals. In both curves, it is seen that the cyclic algorithm achieves better performance, even though its initial convergence is somewhat slower than that of the conventional RLS. Summing up, we can conclude that the conventional algorithm may converge more rapidly than the new algorithm, *but* in many scenarios commonly encountered in mobile communications its steady-state performance is very poor. The cyclic algorithm, instead, even though it converges more slowly, appears more robust, in that it achieves good performance in strong near–far scenarios, as well as in heavily loaded networks; moreover, it is very little affected by abrupt variations in the users number, as witnessed in Fig. 7.

VI. Conclusion

In this paper, the problem of the accommodation of information streams transmitted at one out of two available data rates over an asynchronous DS/CDMA network has been considered. Besides the VSL access scheme, two other access methods have been considered, namely the VCR and the VCRFS, in which users with different data rates are assigned signature waveforms with different bandwidths. Two linear one-shot multiuser receivers—the decorrelating and the MMSE detectors—have been considered, and their performance has been analyzed for all of the three cited access methods.

Furthermore, we have also tackled the problem of blind adaptive detection. We have developed a blind cyclic RLS algorithm which enables blind implementation of the periodically time-varying MMSE high-rate users detector. Such an algorithm has been validated through computer simulations, and its performance assessed also in comparison to the conventional blind RLS algorithm [3].

APPENDIX

In this appendix we briefly illustrate the mathematical details leading from problem (16) to solution (18). First of all, notice that, since the filter $\hat{\boldsymbol{m}}_0(n,i)$ is periodically time-varying in its second argument with period L, it admits the following Fourier expansion:

$$\hat{\boldsymbol{m}}_0(n,i) = \sum_{q=0}^{L-1} \boldsymbol{m}_0^{(q)}(n) \exp\left(j\frac{2\pi qi}{L}\right) \tag{26}$$

with $\{\boldsymbol{m}_0^{(q)}(n)\}_{q=0}^{L-1}$ the coefficients of the Fourier expansion. Substituting (26) into (16) and elaborating leads to the following problem:

$$\begin{cases} \tilde{\boldsymbol{m}}_0^H(n)\tilde{\boldsymbol{R}}(n)\tilde{\boldsymbol{m}}_0(n) = \min \\ \tilde{\boldsymbol{S}}_0^H \tilde{\boldsymbol{m}}_0(n) = \boldsymbol{e}_1 \end{cases} \tag{27}$$

with $\tilde{\boldsymbol{m}}_0(n)$ the $LN^{(h)}M(2V+1)$-dimensional vector of the Fourier coefficients of the filter $\hat{\boldsymbol{m}}_0(n,i)$, i.e.,

$$\tilde{\boldsymbol{m}}_0(n) = \left[\boldsymbol{m}_0^{(0)T}(n), \boldsymbol{m}_0^{(1)T}(n), \ldots, \boldsymbol{m}_0^{(L-1)T}(n)\right]^T$$

and $\tilde{\boldsymbol{R}}(n)$, $\tilde{\boldsymbol{S}}_0$ and $\boldsymbol{e}_1$ are defined in (17) and (19). The problem (27) can now be solved with standard lagrangian techniques, thus yielding the solution

$$\tilde{\boldsymbol{m}}_0(n) = \tilde{\boldsymbol{R}}^{-1}(n)\tilde{\boldsymbol{S}}_0\left(\tilde{\boldsymbol{S}}_0^H\tilde{\boldsymbol{R}}^{-1}(n)\tilde{\boldsymbol{S}}_0\right)^{-1}\boldsymbol{e}_1. \tag{28}$$

Since we are interested to the filter $\hat{\boldsymbol{m}}_0(n,i)$ and not to its Fourier coefficients $\tilde{\boldsymbol{m}}_0(n)$, we have to reconstruct the solution in the time-domain, i.e.,

$$\hat{\boldsymbol{m}}_0(n,i) = \left(\boldsymbol{e}_2^H \otimes \boldsymbol{I}_{N^{(h)}M(2V+1)}\right)\boldsymbol{\Psi}(i)\tilde{\boldsymbol{m}}_0(n) \tag{29}$$

substituting (28) into the above equation, we obtain, after some nontrivial algebraic manipulations

$$\begin{aligned}\hat{\boldsymbol{m}}_0(n,i) &= \frac{\left(\sum_{q=0}^{L-1}\boldsymbol{R}^{(q)}(n)\exp\left(-j\frac{2\pi qn}{L}\right)\right)^{-1}\boldsymbol{s}_{00}}{\boldsymbol{s}_{00}^H\left(\sum_{q=0}^{L-1}\boldsymbol{R}^{(q)}(n)\exp\left(-j\frac{2\pi qn}{L}\right)\right)^{-1}\boldsymbol{s}_{00}} \\ &= \frac{\left(\boldsymbol{e}_2^H \otimes \boldsymbol{I}_{N^{(h)}M(2V+1)}\right)\boldsymbol{\Psi}(i)\tilde{\boldsymbol{R}}^{-1}(n)\tilde{\boldsymbol{S}}_0\boldsymbol{e}_1}{\boldsymbol{s}_{00}^H\left(\boldsymbol{e}_2^H \otimes \boldsymbol{I}_{N^{(h)}M(2V+1)}\right)\boldsymbol{\Psi}(i)\tilde{\boldsymbol{R}}^{-1}(n)\tilde{\boldsymbol{S}}_0\boldsymbol{e}_1}\end{aligned} \tag{30}$$

with $\boldsymbol{R}^{(q)}(n)$ given by (20). In deriving the above expression, we have exploited the following decomposition for the block-circulant matrices $\tilde{\boldsymbol{R}}(n)$ and $\tilde{\boldsymbol{S}}_0$:

$$\tilde{\boldsymbol{R}}(n) = \boldsymbol{E}\boldsymbol{\Lambda}(n)\boldsymbol{E}^H, \quad \tilde{\boldsymbol{S}}_0 = \boldsymbol{E}\tilde{\boldsymbol{S}}_0\boldsymbol{V}^H \tag{31}$$

wherein $\boldsymbol{V} = [\boldsymbol{v}_0, \ldots, \boldsymbol{v}_{L-1}]$ is a square matrix of order L, with $\boldsymbol{v}_i = (1/\sqrt{L})[1, e^{-j(2\pi i/L)}, \ldots, e^{-j((2\pi(L-1)i)/L)}]^T$, while $\boldsymbol{E} = [\boldsymbol{E}_0, \ldots, \boldsymbol{E}_{L-1}]$ is a square matrix of order $LMN^{(h)}(2V+1)$ with $\boldsymbol{E}_i = \boldsymbol{v}_i \otimes \boldsymbol{I}_{N^{(h)}M(2V+1)}$. Finally, $\boldsymbol{\Lambda}(n)$ is the following block-diagonal square matrix of order $LMN^{(h)}(2V+1)$:

$$\boldsymbol{\Lambda}(n) = \mathrm{Diag}\left(\boldsymbol{\Lambda}^{(0)}(n), \ldots, \boldsymbol{\Lambda}^{(L-1)}(n)\right)$$

with $\boldsymbol{\Lambda}^{(i)}(n) = \sum_{q=0}^{L-1}\boldsymbol{R}^{(q)}(n)e^{j(2\pi qi/L)}$. Decompositions (31) may be obtained by generalizing to block-circulant matrices the properties of circulant matrices reported in [27]. We do not give proofs of their validity for sake of brevity.

Based on the matrix inversion lemma [21], it can be easily shown that solution (30) can be recursively implemented through procedure (18).

REFERENCES

[1] S. Verdú, *Multiuser Detection*, Cambridge, U.K.: Cambridge University Press, 1998.

[2] M. Honig, U. Madhow, and S. Verdú, "Blind adaptive multiuser detection," *IEEE Trans. Inform. Theory*, vol. 41, pp. 944–960, July 1995.

[3] H. V. Poor and X. Wang, "Code-aided interference suppression for DS/CDMA communications—Part I: Interference suppression capability, part II: Parallel blind adaptive implementations," *IEEE Trans. Commun.*, vol. 45, pp. 1101–1122, Sept. 1997.

[4] X. Wang and H. V. Poor, "Blind multiuser detection: A subspace approach," *IEEE Trans. Inform. Theory*, vol. 44, pp. 677–690, Mar. 1998.

[5] E. Dahlman, B. Gudmundson, M. Nilsson, and J. Sköld, "UMTS/IMT-2000 based on wideband CDMA," *IEEE Personal Commun. Mag.*, vol. 36, pp. 70–80, Sept. 1998.

[6] C.-L. I and R. D. Gitlin, "Multi-code CDMA wireless personal communications networks," presented at the IEEE Int. Conf. Comm., Seattle, WA, June 1995.

[7] U. Mitra, "Comparative study of maximum likelihood detection for two multi-rate DS/CDMA systems," presented at the Int. Symp. Inform. Theory, Ulm, Germany, June 1997.

[8] ——, "Comparison of maximum likelihood-based detection for two multi-rate access schemes for CDMA signals," *IEEE Trans. Comm.*, vol. 47, pp. 64–77, Jan. 1999.

[9] M. Saquib, R. Yates, and N. Mandayam, "Decorrelating detectors for a dual rate synchronous DS/CDMA channel," *Wireless Pers. Commun.*, vol. 9, pp. 197–216, May 1999.

[10] J. Chen and U. Mitra, "Further results for multi-rate decorrelators for synchronous DS/CDMA systems," presented at the 34th Annu. Allerton Conf. Commun., Contr. Computing, Oct. 1996.

[11] ——, "MMSE receivers for dual-rate DS/CDMA signals: Random signature sequence analysis," presented at the Globecom, Phoenix, AZ, Nov. 1997.

[12] H. Ge, "Multiuser detection for integrated multi-rate CDMA," presented at the 1st Int. Conf. Inform., Commun. Signal Processing, Singapore, Sept. 1997.

[13] M. Saquib, R. Yates, and N. Mandayam, "A decision feedback decorrelator for a dual rate synchronous DS/CDMA channel," *ACM Wireless Networks J.*, vol. 4, no. 6, pp. 497–506, 1998.

[14] T.-H. Wu and E. Geraniotis, "CDMA with multiple chip rates for multimedia communications," presented at the 28th Annu. Conf. Inform. Sci. Syst., Princeton, NJ, Mar. 1994.

[15] S. Buzzi, M. Lops, and A. M. Tulino, "MMSE multi-user detection for asynchronous dual rate direct sequence CDMA communications," presented at the 9th Int. Symp. Personal Indoor Mobile Radio Commun., Boston, MA, Sept. 8–11, 1998.

[16] P. Taaghol, B. G. Evans, R. De Gaudenzi, G. Gallinaro, J. H. Lee, and C. G. Kang, "Satellite UMTS/IMT200 W-CDMA air interfaces," *IEEE Commun. Mag.*, vol. 37, pp. 116–126, Sept. 1999.
[17] M. Juntti and J. O. Lilleberg, "Linear FIR multiuser detection for multiple data-rate CDMA systems," presented at the 47th IEEE Veh. Technol. Conf., Phoenix, AZ, May 1997.
[18] E. G. Ström, S. Parkvall, S. L. Miller, and B. E. Ottersten, "Propagation delay estimation in asynchronous direct-sequence code-division multiple access systems," *IEEE Trans. Commun.*, vol. 44, pp. 84–93, Jan. 1996.
[19] M. Lops, G. Ricci, and A. M. Tulino, "Narrowband interference suppression in multiuser CDMA systems," *IEEE Trans. Commun.*, vol. 46, pp. 1163–1175, Sept. 1998.
[20] S. Buzzi, M. Lops, and A. M. Tulino, "Time-varying narrowband interference rejection in asynchronous multiuser DS/CDMA systems over frequency-selective fading channels," *IEEE Trans. Commun.*, vol. 47, pp. 1523–1536, Oct. 1999.
[21] G. H. Golub and C. F. Van Loan, *Matrix Computations*, 2nd ed. Baltimore, MD: The John Hopkins Univ. Press, 1990.
[22] U. Madhow and M. L. Honig, "MMSE interference suppression for direct-sequence spread-spectrum CDMA," *IEEE Trans. Commun.*, vol. 42, pp. 3178–3188, Dec. 1994.
[23] K. Fukawa and H. Suzuki, "Orthogonalizing matched filtering (OMF) detector for DS-CDMA mobile communication systems," *IEEE Trans. Veh. Technol.*, vol. 48, pp. 188–196, Jan. 1999.
[24] W. A. Gardner, *Introduction to Random Processes with Applications to Signals and Systems*. New York: Macmillan, 1986.
[25] S. Haykin, *Adaptive Filter Theory*, 3rd ed. Englewood Cliffs, NJ: Prentice-Hall, 1996.
[26] R. B. Ash, *Real Analysis and Probability*. New York: Academic, 1972.
[27] P. Lancaster, *The Theory of Matrices with Applications*. New York: Academic, 1985.

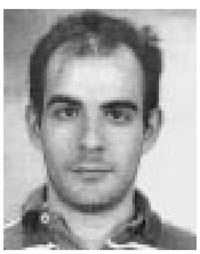

Stefano Buzzi (M'98) was born in Piano di Sorrento, Italy, on December 10, 1970. He received (with honors) the Dr.Eng. degree in 1994, and the Ph.D. degree in electronic engineering and computer science in 1999, both from the University of Naples "Federico II."

In 1996, he spent six months at Centro Studi e Laboratori Telecomunicazioni (*CSELT*), Turin, Italy, where he was introduced to high speed networks. During 1999–2000, he was with the Department of Electrical Engineering, Princeton University, Princeton, NJ, as a Visiting Research Fellow. He is currently an Assistant Professor with the University of Cassino, Italy. His current research and study interests lie in the area of statistical signal processing, with emphasis on signal detection in nongaussian noise and multiple access communications.

Dr. Buzzi was awarded by the AEI (Associazione Elettrotecnica ed Elettronica Italiana) the "G. Oglietti" scholarship in 1996, and was the recipient of a NATO/CNR advanced fellowship in 1999.

Marco Lops (M'96) was born in Naples, Italy, on March 16, 1961. He received the Dr.Eng. degree in electronic engineering from the University of Naples in 1986 and the Ph.D. degree in electronic engineering from the University of Naples in 1992.

From 1986 to 1987, he was with Selenia, Rome, Italy as an Engineer in the Air Traffic Control Systems Group. From 1991 to 2000, he has been an Associate Professor of Radar Theory and Digital Transmission Theory with the University of Naples. Since March 2000, he has been a Full Professor with the University of Cassino, engaged in research in the field of statistical signal processing, with emphasis on radar processing and spread spectrum multiuser communications. He also held teaching positions at the University of Lecce; and during 1991 and 1998, he was on sabbatical leaves at University of Connecticut, Storrs, CT and Rice University, Houston, TX, respectively.

Antonia M. Tulino was born in Naples, Italy, on September 12, 1971. She received (with honors) the Dr.Eng. degree from the Università degli Studi di Napoli "Federico II," Italy, in 1995, and the Ph.D. degree in electronic engineering from the Seconda Università degli Studi di Napoli, Italy, in 1999.

In 1999, she was a Research Scientist with the Center for Wireless Communications (CWC), Oulu, Finland. She is currently a Postdoctoral Visiting Researcher at Princeton University, Princeton, NJ. Her current research and study interests lie in the area of statistical signal processing, with emphasis on code division multiple access systems.